X-ray focusing test and x-ray imaging test by a microcapillary x-ray lens at an undulator beamline

Yoshiki Kohmura
SPring-8, Harima Institute, The Institute of Physical and Chemical Research (RIKEN), Kouto 1-1-1, Mikazuki-cho, Sayo-gun, Hyogo, 679-5148, Japan

Mitsuhiro Awaji and Yoshio Suzuki
SPring-8, Japan Synchrotron Radiation Research Institute (JASRI), Kouto 1-1-1, Mikazuki-cho, Sayou-gun, Hyogo, 679-5198, Japan

Tetsuya Ishikawa
SPring-8, Harima Institute, The Institute of Physical and Chemical Research (RIKEN), Kouto 1-1-1, Mikazuki-cho, Sayo-gun, Hyogo, 679-5148, Japan and SPring-8, Japan Synchrotron Radiation Research Institute (JASRI), Kouto 1-1-1, Mikazuki-cho, Sayou-gun, Hyogo, 679-5198, Japan

Yu. I. Dudchik, N. N. Kolchevsky, and F. F. Komarov
Institute of Applied Physics Problems, Kurchatova 7, Minsk 220064, Belarus

(Received 28 April 1999; accepted for publication 26 July 1999)

A first focusing test of the undulator radiation at SPring-8 has been done using two types of x-ray refractive lenses in thin glass capillaries. One (lens No. 1) contained bubbles in a glue whereas the other (lens No. 2) contained bubbles in glycerol. The capillaries had inner diameters of 0.2 and 0.8 mm, respectively. Using x rays of 17–18 keV, the undulator source image was investigated at the focal plane. The spherical aberrations and the field distortions were carefully examined by taking the images of a gold mesh. Lens No. 1 had an advantage of high transmissivity in the hard x-ray region (18% at 18 keV) and high tolerance to severe radiation damage, e.g., $\sim 5\times 10^{12}$ photons/s/0.03 mm^2 of the 18 keV x rays for an exposure time of 1 h. On the other hand, lens No. 2 had an advantage of a large aperture, 0.8 mm, and a small field distortion, e.g., less than 10% inside a diameter of 300 μm. © *1999 American Institute of Physics.* [S0034-6748(99)05011-X]

I. INTRODUCTION

Due to the extremely small refractive index decrement of x rays ($\delta \sim 10^{-6}$, $n=1-\delta+i\beta$, where n and β are the refractive index and absorption index, respectively), an x-ray refractive lens has been unrealistic until recently. An x-ray refractive lens using a high-atomic number (high-Z) material has been proposed by Suehiro, Miyaji, and Hayashi for focusing undulator radiation,[1] but a long beamline of about 1 km would be needed. Yang[2] proposed the idea of a lens made of low-Z material for focusing hard x rays without much absorption, but the lens radii, a few micrometer, were too small. An x-ray refractive lens has been realized for the first time by Snigirev *et al.* by producing a linear array of many cylindrical lenses (compound refractive lens.)[3] Two-dimensional lenses were also developed by crossing two linear arrays in perpendicular directions.[4] The maximum gain obtained by these two-dimensional lenses, however, was reported[4] to be around 15 and there is much room for improvement. The number of pinholes for this kind of two-dimensional lens needs to be twice larger than the one-dimensional one and absorption of the x rays through the bridges becomes unnecessarily large. To minimize the effect by x-ray absorption and by small angle scattering, materials such as beryllium were also extensively tested.[5,6]

At SPring-8, an array of one-dimensional lenses was evaluated as the ''collimator'' of the undulator beam. They were fabricated on plastics or beryllium plates and their focal lengths were chosen to be close to the distance between the x-ray source and the lens (e.g., ~45 m).[7,8] Such ''collimators'' would be useful for high-angular and high-energy resolution experiments such as inelastic scattering and nuclear scattering experiments.[7,8]

In order to improve the gain, a refractive lens with an array of spherical or parabolic lenses[6] is preferable. Many technical difficulties, however, exist for realizing such forms on metallic materials by precise machining. On the other hand, when liquids and gases are used as the lens material, the surface tension helps to realize spherical and parabolic shapes much more naturally.

The so-called ''bubble lens'' and ''hollow plastic ball lens'' were manufactured where bubbles on an adhesive liquid[9] and hollow plastic balls on pure water[10,11] were placed in order to realize the spherical interfaces between air and the lens materials. The diameters of the bubbles and the inner diameters of the hollow plastic balls were about 2 and 1.7 mm, respectively.[9]

Here, we report the results from the first test of the ''microcapillary lens''[12] developed at the Institute of Applied Physics Problems, Belarus. An undulator beamline, BL47, at SPring-8 was used for the experiment. The first type of the lens (No. 1) was produced by forming bubbles in a glue inside in a thin glass capillary and was solidified to obtain a solid x-ray refractive lens.[12] Presently, a lens with a diameter as large as 1–2 mm can not be fabricated. Therefore, the

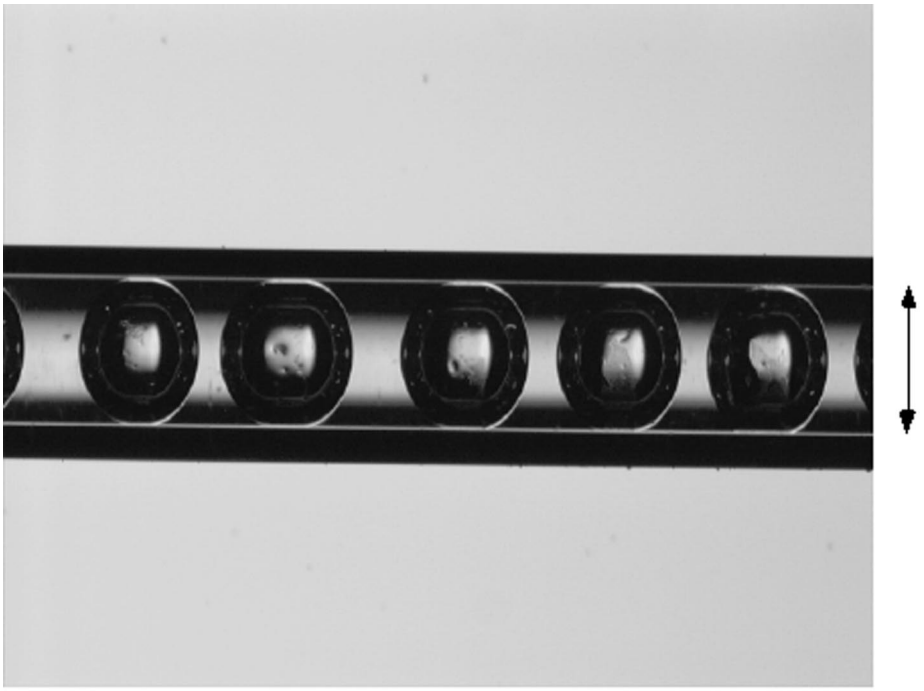

FIG. 1. Magnified image of lens No. 2 using a visible light microscope. Inner diameter of the glass capillary is 800 nm.

bubbles were formed in glycerol in the second type of the lens (No. 2). For both of these lenses, the surface tension of the liquid inside the glass forces the surface to have an approximately spherical shape. The lenses investigated had inner diameters of about 0.2 mm (No. 1) and 0.8 mm (No. 2), respectively. Using x-rays of 16.5–18.3 keV, the lens quality was investigated in terms of the focus size, the gain, and the transmissivity, and the spherical aberration effects were carefully examined by taking the images of the gold mesh.

II. METHODS FOR EVALUATING THE LENSES

The evaluation of the ''microcapillary lens'' was done at BL47 of SPring-8 (Ref. 13) using the standard in-vacuum undulator[14,15] and a cryogenically cooled Si monochromator, which could tolerate the full heat load from the undulator with a small gap.[16] First, the demagnified image of the undulator source was taken and the source image was evaluated in terms of the image size, the gain around the focal plane. Most of the measurements were done for the lens No. 1, which has a length $L=59$ mm and inner radius $r=0.10$ mm with the number of microlenses $N=71$. Second, the magnified image of a gold mesh was taken in order to examine the spherical aberration. This measurement was done for the lens Nos. 1 and 2. Lens No. 2 has a length $L=225$ mm and inner radius $r=0.4$ mm with the number of microlenses $N=185$. The magnified image of the lens No. 2 using the visible light microscope is shown in Fig. 1.

A. Evaluating the source image at the focal plane

The source image of the undulator radiation (with a gap of 40 mm) was taken and investigated mainly for lens No. 1 at the x-ray energy of 18.3 keV. The undulator source size in full width at half maximum (FWHM) was expected to be about 800 μm$\times$30 μm (assuming a coupling constant of 0.15%). The focal length of this lens was expected to be about 1 m and the focus image of the source was expected to be formed at about this length downstream of the lens because the distance between the source and the lens, about 45 m, was much larger than the focal length. Therefore, the expected geometrical demagnification factor was about 1/45. However, a spherical aberration needs to be taken into consideration. By the ray-trace simulation described later, the image size at a focus in FWHM was expected to be $\leqslant 2$ μm and about 18 μm in the vertical and horizontal directions.

By experiment, the focus position was determined by measuring the vertical profiles at different positions along the optical axis. These measurements were done with a wire scan (a kind of a knife-edge scan) technique (Fig. 2). This scan was carried out with a precision of better than 0.1 μm. A diaphragm (with diameter of 200 μm) was closely placed downstream of the lens to exclude the x rays outside the aperture of the lens.

The gain was measured by comparison of the brightness with and without the lens. In principle, a two-dimensional brightness distribution is needed to be measured with a spatial resolution of 1 μm or so. The spatial resolutions of most of our position-sensitive detectors were worse than this criterion and the x-ray films and nuclear plates were not suitable because of their poor linearity to the incident intensity. Another solution for such measurement can be considered by scanning a pinhole or a slit with a diameter or width of less than 1 μm or so. Experiments with such pinholes and slits, however, are also difficult in the x-ray region.

The gain, here, was measured in the following way. A charge-coupled device camera (Hamamatsu Photonics, C4880-17) with a phosphor screen and a relay lens (hereaf-

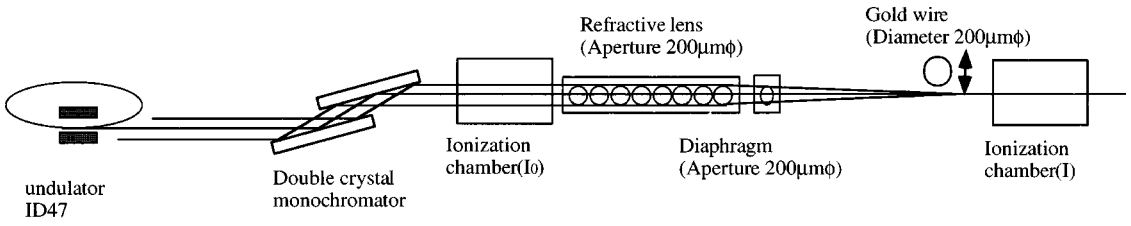

FIG. 2. Experimental setup for measuring the focus size using a wire scan and for measuring the transmissivity of the lens. An ionization chamber was used as the detector and a gold wire with a diameter of 200 μm was used. 18.3 keV x rays were utilized and a diaphram (with a diameter of 200 μm) was closely placed downstream of the lens to exclude the x rays outside the aperture of the lens.

ter, ''beam monitor'') was used to record the x-ray image. The relay lens magnifies the fluorescence light from the phosphor screen by a magnification factor of 2. The visibility of the gold mesh observed with this detector showed that the spatial resolution of this detector was about 10 μm. On the other hand, a wire scan measurement was done with a step of 0.5 μm. Through this measurement, a much more precise intensity profile can be obtained. The projected one-dimensional profiles by the ''beam monitor'' (in the vertical and horizontal directions) were deconvolved to have the same profile as the wire scan data (summed over an area of the pixel size of the ''beam monitor''), while the renormalization factor was chosen to conserve the total integrated intensity.

The transmissivity of the lens was measured with an air-filled ionization chamber as the ratio of the currents with and without the lens (Fig. 2). A diaphragm with a diameter of 200 μm was closely placed downstream of the lens to exclude the x rays outside the aperture of the lens.

B. Evaluating the magnified image of a gold mesh

To visualize the spherical aberration and the field distortion, it is convenient to take the images of a mesh and see the distortions from the lattice. The undulator gap was as set to 44 mm for this experiment. A gold mesh was placed upstream of the lens and the distances from the lens to the detector were set to 3.6 and 5 m, for lens Nos. 1 and 2, respectively (Fig. 3). Since the focal lengths of the lens Nos. 1 and 2 were around 0.9 m (at 18.3 keV) and 1.2 m (at 17.1 keV), images with magnification factors of around 3 and 3.2 could be obtained, respectively. As for the mesh, a gold mesh manufactured by the Good Fellow Co., Britain, was used which had a wire diameter of 5.6 μm with a thickness of $\sim$5 μm with a pitch of 16.7 μm.

C. Ray-trace simulations

The results of the experiments were compared with ray-trace simulations assuming perfectly spherical microlenses. For the calculations, parallel incident x-ray beams were assumed while the incident beam from the undulator is quasi-parallel (with divergences of $\sigma_{x'}=18$ μrad and $\sigma_{y'}=8$ μrad at an x-ray energy of $\sim$ 18 keV). As for the experiment with the gold mesh, the diffraction and the scattering intensities are small at the gold wires and the mesh work, in a good approximation, as a mask along the parallel x-ray beam which does not change the direction of the incident x rays.

III. RESULTS OF THE EXPERIMENTS

A. Source image at the focal plane

The focal length was determined by repeating the wire scans at various positions from lens No. 1. The vertical intensity profiles were measured with a gold wire at distances from the lens L_2 of 0.6, 0.7, 0.8, and 0.9 m [Figs. 4(a), 4(b), 4(c) and 4(d)]. Each scan was done at a step of 0.5 μm with an integration time of 1 s. The horizontal profile was measured only at L_2 of 0.8 m, which seemed to be reasonably near the focal plane [Fig. 4(e)]. A low-frequency source movement in a few Hz appeared as oscillations at the tail around the focus spot.

The vertical profile at $L_2=0.6$ and 0.7 m showed a rather flat top which indicated that L_2 is smaller than the focal

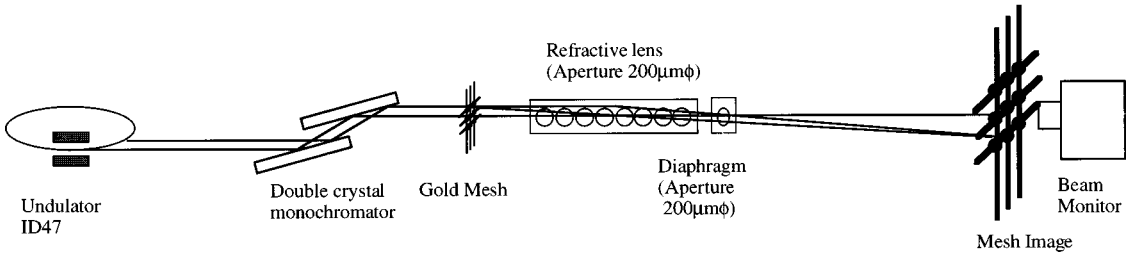

FIG. 3. Experimental setup for taking images of the gold mesh. Images with magnification factors of around 3 and 3.2 were obtained for lens Nos. 1 and 2, respectively, by placing the gold mesh upstream of the lens and placing the detector at about 3.6 and 5 m downstream of the lens Nos. 1 and 2, respectively. A gold mesh manufactured by the Good Fellow Co., Britain, was used which had a wire diameter of 5.6 μm with a thickness of $\sim$5 μm and a pitch of 16.7 μm.

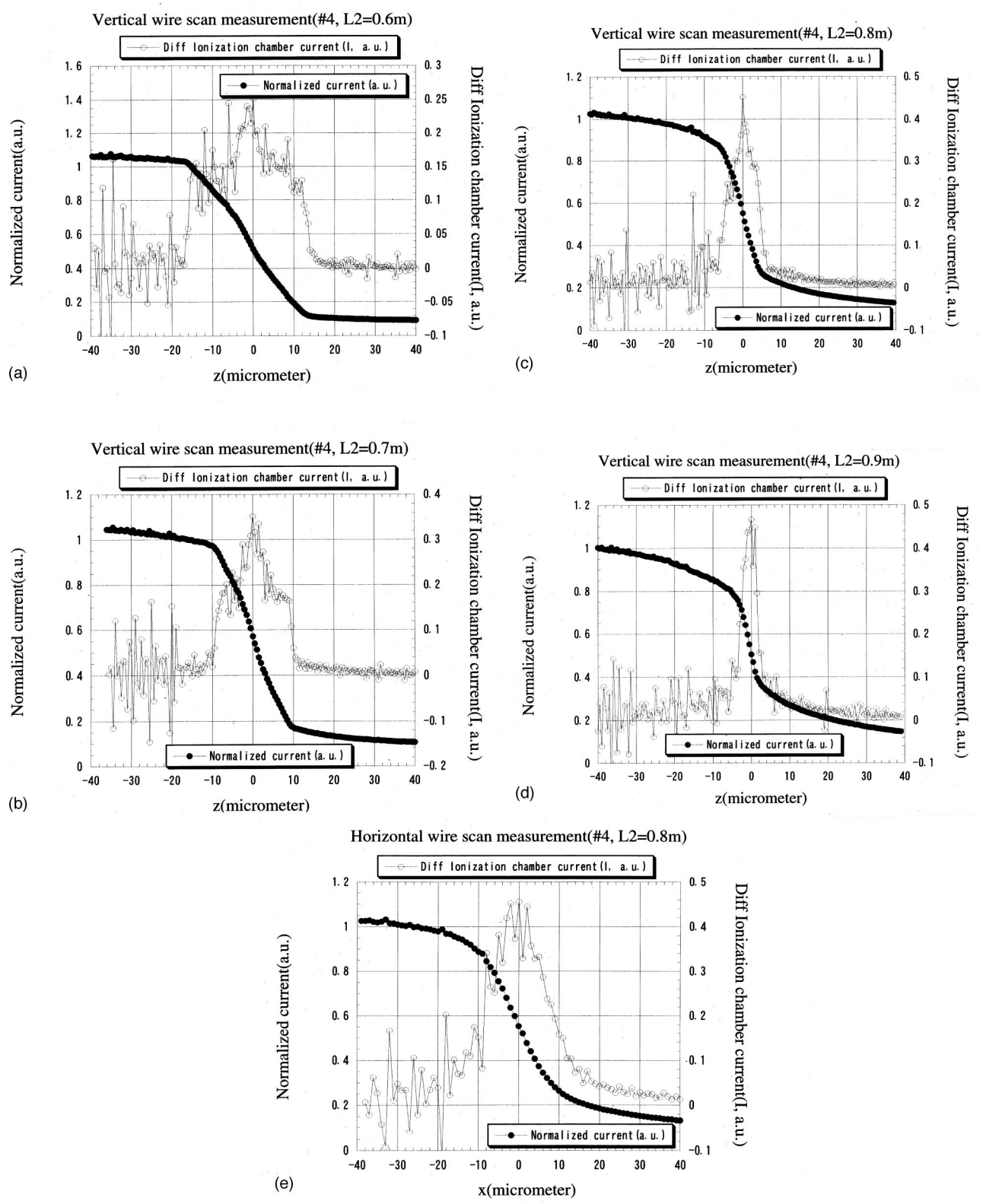

FIG. 4. Result of the measurements of the intensity distributions at various distances from the lens No. 1. Wire scan measurements in the vertical direction of the gold wire with a diameter of 200 μm were done and the raw data together with the differenciated profiles are shown for (a) $L_2=0.6$ m, (b) 0.7 m, (c) 0.8 m, and (d) 0.9 m, where L_2 stands for the distance between the lens and the wire. A wire scan measurement in the horizontal direction for (e) $L_2=0.8$ m is also shown.

length. On the other hand, the tail structure became apparent as L_2 was increased from 0.8 to 0.9 m. Nearly 60% of the total flux was involved in the central peak at $L_2=0.8$ m which decreased to 40% at $L_2=0.9$ m. The focus size measured was 8 μm both for $L_2=0.8$ and 0.9 m. We searched for a smaller spot size (in the vertical direction) around the focal plane but we could not obtain a small spot size of less than 2 μm as the ray-trace simulations suggested. We did experi-

ment with a tiny pinhole (50 μm ϕ) just in front of the lens to reduce the off-axis flux and to reduce the spherical aberration, but the focus size was not reduced significantly. We, therefore, concluded that the lens is not so perfect and detailed model fitting would not be needed. This may be caused by the deformation of the bubbles from perfect spheres. Though the focal condition seemed to be at $L_2\sim$ 1 m, assuming the inner radius of the capillary ($R=0.104$ mm) and the number of the microlenses ($N=71$), we concluded that the focus position exists somewhere between $L_2=0.8$ and 0.9 m. The sizes of the focus was evaluated at $L_2=$ 0.8 m to be about 16 μm$\times$8 μm (horizontal FWHM$\times$vertical FWHM). As the undulator source size in the FWHM was expected to be about 800 μm$\times$30 μm (assuming a coupling constant of 0.15%), the observed image size agreed with the expected one in the horizontal direction (assuming a demagnification factor of 1/50), but it was much larger than expected in the vertical direction ($\leqslant$2 μm, according to ray-trace simulations). The observed focal length, suggests that microlenses may not be perfect spheres with the assumed radius of 0.10 mm and the ''effective'' radius could have been 0.09 mm.

The beam profile was observed with and without the lens by the ''beam monitor.'' From the ratio of the peak intensities observed by this detector, the gain was calculated to be about 3.3. But this gain is affected by the finite resolution (about 10 μm) of the detector as described in Sec. II A. We deconvolved the one-dimensional projections by renormalizing the wire scan data in the vertical and horizontal directions. From this deconvolution, the true gain was calculated to be about 12. The transmissivity of the lens was carefully determined by the ratio of the flux through the entrance pupil with and without the lens. The measured value for the transmissivity was about 18% at an energy of 18.3 keV.

B. Magnified image of a gold mesh

The expected transmission through the gold wire was 0.39 at an x-ray energy of 18.3 keV (corresponding to a thickness of about 5 μm). This corresponds to a visibility of 0.44. When this mesh was closely placed in front of the beam monitor, the visibility $[(I_{\max}-I_{\min})/(I_{\max}+I_{\min})]$, however, was measured to be about 0.07 due to the finite spatial resolution of the detector ($\sim$10 μm). $I_{\max}$ and $I_{\min}$ here represent the maximum and the minimum intensities around the dips caused by the gold wires, respectively.

The mesh image (at 18.3 keV) was taken using lens No. 1 and is shown in Fig. 5(a). This apparently shows the curvature of field due to the spherical aberration. A ray-tracing simulation was also done for this measurement assuming perfect spherical microcapillary lenses with a focal length of 0.9 m. Figure 5(b) shows the observed image and the calculated one overlapped, which show a close resemblance.

Mesh images were taken at various x-ray energies (16.5–18.1 keV) using lens No. 2 and the visibilities were measured at various wire positions. The positions of the lens and the beam monitor were fixed (the distance from the lens to the mesh being $\sim$2 m and to the beam monitor being $\sim$5 m, respectively). Figure 6(a) shows the image obtained at 17.1 keV. The shadows of the wire became clear at 17.1 keV

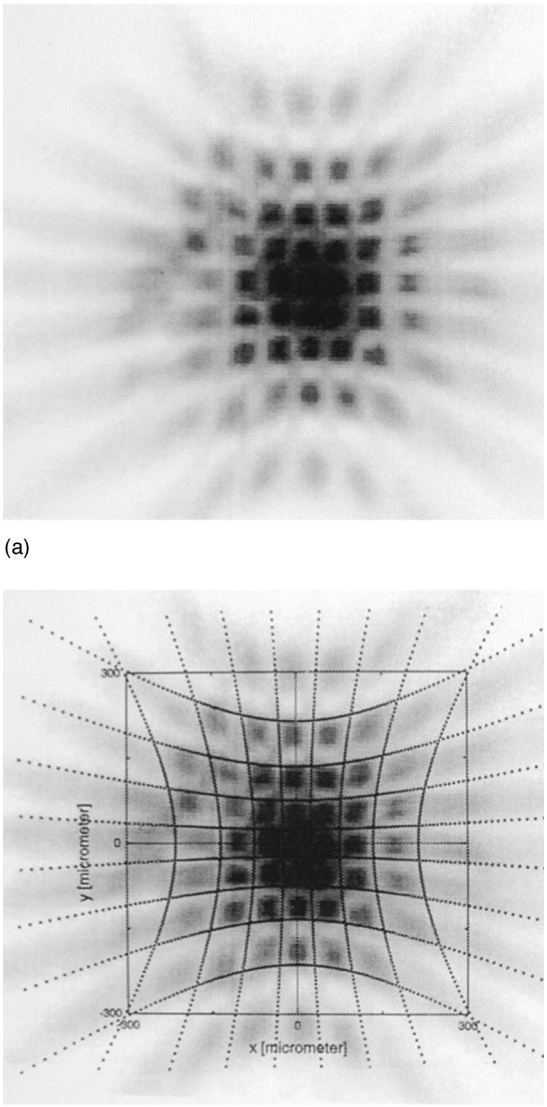

(a)

(b)

FIG. 5. (a) Image of a gold mesh (Good Fellow Co.) using lens No. 1 with a magnification factor of about 3 at an x-ray energy of 18.3 keV (the distances between the mesh and lens and between the lens and the detector were chosen to be 1.2 and 3.6 m, respectively). (b) Simulated mesh image by a ray-trace calculation and the observed image overlapped. The distortion from the lattice was well reproduced in the simulation.

and the visibility for the near-axis wires approached the expected value of $\sim$0.4 at this energy. The fine wires were barely seen without the lens, but magnification by $\sim$3.2 enlarged the wire diameters and the pitches to about 16 and 53 μm, respectively, and made these wires easily resolved by the detector (with a spatial resolution of $\sim$10 μm).

Figure 6(b) shows the observed image and the calculated one overlapped. In this case, the focal length of the lens was assumed to be 1.2 m. Figure 6(b) again shows the resemblance of the observed mesh image and the simulated one. The focal lengths (calculated from the separation of the wires) roughly changed proportional to the square of the x-ray energy as theoretically expected. The curvature of field of the image was much reduced compared to lens No. 1 due to the larger radii of curvature of the lens.

The position linearity of the image was investigated by

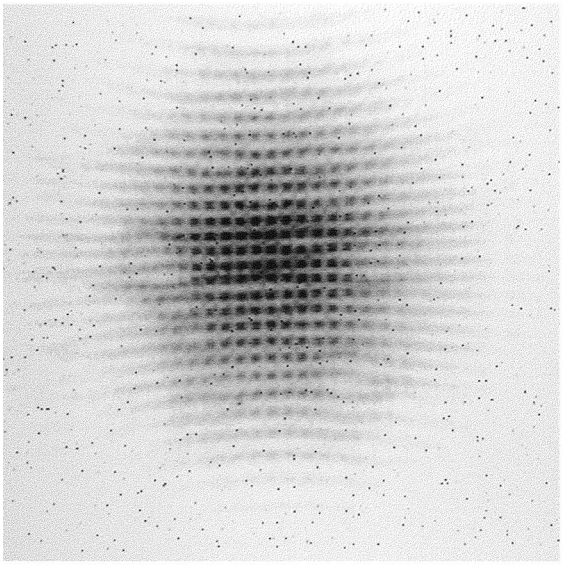

(a)

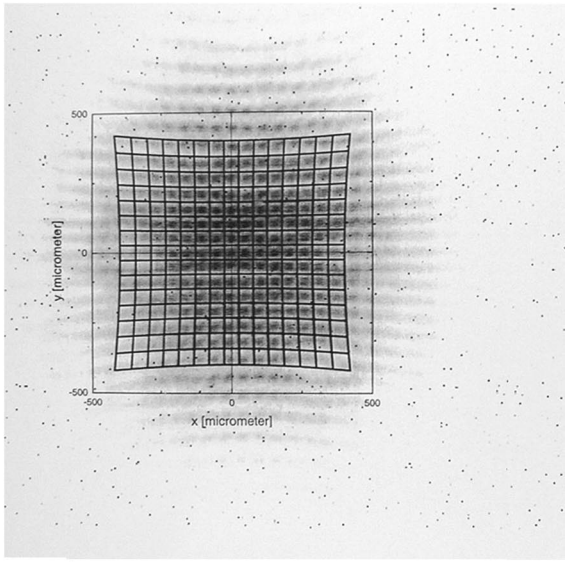

(b)

FIG. 6. (a) Image of a gold mesh (Good Fellow Co.) using lens No. 2 with a magnification factor of about 3.2 at an x-ray energy of 17.1 keV. (b) Simulated mesh image by a ray-trace calculation and the observed image overlapped. The distortion from the lattice was well reproduced in the simulation.

measuring the distortion of the mesh image from the lattice. The distortion was less than 10% inside a diameter of 300 μm.

C. Test of radiation damage

Lens No. 1 was formed with glues and the stability of the glue was not known. To check the stability in an extremely high x-ray flux and a high radiation damage, a lens with the same ingredient as lens No. 1 was placed into the optical axis. This experiment was also done at BL47XU of SPring-8 with an undulator gap of 10 mm (near the minimum of 8 mm). The monochromator was set so that the third-order harmonics, 18 keV, were transmitted into the experimental station. The lens was adjusted to the x-ray optical

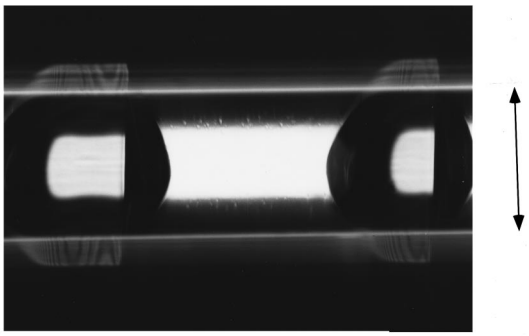

(a)

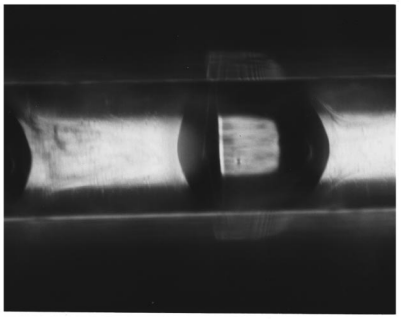

(b)

FIG. 7. Result of the radiation damage test for the lens material (glue) of lens No. 1. A high x-ray flux density of $\sim 5\times 10^{12}$ photons/s/0.03 mm^2 was illuminated onto the lens with the exposure time of 1 h. Visible light microscope image of the most upstream part of the lens (a) before exposure and (b) after exposure. Inner diameter of the glass capillary is 350 nmϕ.

axis and a flux density of $\sim 5\times 10^{12}$ photons/s/0.03 mm^2 was expected to be illuminated on the lens. The exposure time was 1 h.

After the 1 h exposure, the most upstream part of the lens, composed of glue, was discolored. The glue turned yellow from its initial color of dark green and small density fluctuations were seen, as shown in Fig. 7. Only two microlenses (the glue parts for a length of about 2 cm) were affected by this effect. Therefore, the focusing capability seemed not to be affected so much.

IV. DISCUSSION

A first focusing test using the undulator radiation of SPring-8 has been done for two types of x-ray refractive lens in thin glass capillaries. One (lens No. 1) contained bubbles in a glue whereas the other (lens No. 2) contained bubbles in glycerol inside a glass capillary with inner diameters of 0.2 and 0.8 mm, respectively. Using x rays of 18.3 keV, the undulator source image was investigated at the focal plane in terms of the focus size, the gain, and the transmissivity (for lens No. 1). The spherical aberrations and field distortions were carefully examined by taking the images of the gold mesh (for lenses Nos. 1 and 2).

For both lenses, the images of the gold mesh showed close resemblances to that obtained from ray-trace calculations assuming perfect spherical microlenses. This fact suggested that the ''microcapillary lens'' reported here is suitable for fabricating a series of spherical microlenses. It has

an advantage of high transmissivity in the hard x-ray region (e.g., 18% at an energy of 18 keV for lens No. 1).

However, there were several aspects in which the microcapillary lens was not so perfect. For example, lens No. 1 showed that (i) the vertical source image size obtained at the focal plane of the lens was about 8 μm in the vertical direction, while the expected size was less than 2 μm (whereas the horizontal size, 16 μm, agrees with the calculations); (ii) the observed gain was no more than about 12 at an x-ray energy of 18 keV; and (iii) some irregularity of the mesh image was seen. These possibilities indicate slope error, deformation of the bubbles from perfect spheres or an inhomogeneity in the lens material. However, the effect of a slight bend of the monochromator crystal planes can be different in the vertical and horizontal directions. Such a bend can be caused by the way crystals were held, or by the heat load of the undulator radiation (though it is less than 10 W with an undulator gap of 40 mm).

Lens No. 1 was found to tolerate severe radiation damage. This lens was not severely damaged with a high x-ray flux ($\sim 5\times 10^{12}$ photons/s/0.03 mm^2) of 18 keV x rays for an exposure time of 1 h.

As for a lens with a larger aperture (lens No. 2), the difference of the focus condition at different energies (16.5–18.1 keV) was investigated in terms of the visibility of the gold wire with fixed positions of the mesh, lens, and detector. The position linearity for this lens was investigated by measuring the distortion of the mesh image from the lattice. The distortion was found to be less than 10% inside a diameter of 300 μm.

Reducing the distortions of the image will be achieved by lenses having larger apertures or with parabolic lenses. Larger apertures will also increase the total flux in the focal spot.

ACKNOWLEDGMENTS

The synchrotron radiation experiments were performed at the SPring-8 with the approval of the Japan Synchrotron Radiation Research Institute (JASRI) (Proposal No. 1998A0161-NM-np). The authors thank A. Baron for helpful discussions.

[1] S. Suehiro, H. Miyaji, and H. Hayashi, Nature (London) **352**, 385 (1991).
[2] B. X. Yang, Nucl. Instrum. Methods Phys. Res. A **328**, 578 (1993).
[3] A. Snigirev, V. Kohn, I. Snigireva, and B. Lengeler, Nature (London) **384**, 49 (1996).
[4] P. Elleaume, J. Synchrotron Radiat. **5**, 1 (1997).
[5] A. Snigirev, V. Kohn, I. Snigireva, A. Souvorov, and B. Lengeler, Appl. Opt. **37**, 653 (1998).
[6] B. Lengeler, J. Tummer, A. Snigirev, I. Snigireva, and C. Raven, J. Appl. Phys. **84**, 5855 (1998).
[7] A. Q. R. Baron, Y. Kohmura, Y. Ohishi, and T. Ishikawa, Appl. Phys. Lett. **74**, 1492 (1999).
[8] A. Q. R. Baron, V. V. Krishnamurthy, Y. Kohmura, Yu. V. Shvyd'ko, and T. Ishikawa, J. Synchrotron Radiat. **6**, 953 (1999).
[9] Y. Kohmura, M. Awaji, Y. Suzuki, and T. Ishikawa, Proc. SPIE **3449**, 185 (1998).
[10] M. Takagi, T. Norimatsu, Y. Yamanaka, and S. Nakai, J. Vac. Sci. Technol. A **9**, 2145 (1991).
[11] M. Takagi, M. Ishihara, T. Norimatsu, T. Yamanaka, Y. Izawa, and S. Nakai, J. Vac. Sci. Technol. A **11**, 2837 (1993).
[12] Yu. I. Dudchik and N. N. Kolchvsky, Nucl. Instrum. Methods Phys. Res. A **421**, 361 (1999).
[13] Y. Kohmura, Y. Suzuki, and T. Ishikawa, SPring-8 User Information Newsletter **3**(4), 28 (1998) (in Japanese).
[14] H. Kitamura, J. Synchrotron Radiat. **5**, 184 (1998).
[15] T. Hara, T. Tanaka, T. Tanabe, X.-M. Marechal, S. Okada, and H. Kitamura, J. Synchrotron Radiat. **5**, 403 (1998).
[16] T. Mochizuki (unpublished).